Laser-Induced Rotation of Iodine Molecules in Helium Nanodroplets: Revivals and Breaking Free

Benjamin Shepperson,[1] Anders A. Søndergaard,[2] Lars Christiansen,[1] Jan Kaczmarczyk,[3]
Robert E. Zillich,[4,*] Mikhail Lemeshko,[3,†] and Henrik Stapelfeldt[1,‡]
[1]*Department of Chemistry, Aarhus University, 8000 Aarhus C, Denmark*
[2]*Department of Physics and Astronomy, Aarhus University, 8000 Aarhus C, Denmark*
[3]*IST Austria (Institute of Science and Technology Austria), Am Campus 1, 3400 Klosterneuburg, Austria*
[4]*Institute for Theoretical Physics, Johannes Kepler Universität Linz, Altenbergerstraße 69, A-4040 Linz, Austria*

(Received 1 February 2017; published 19 May 2017)

Rotation of molecules embedded in helium nanodroplets is explored by a combination of fs laser-induced alignment experiments and angulon quasiparticle theory. We demonstrate that at low fluence of the fs alignment pulse, the molecule and its solvation shell can be set into coherent collective rotation lasting long enough to form revivals. With increasing fluence, however, the revivals disappear—instead, rotational dynamics as rapid as for an isolated molecule is observed during the first few picoseconds. Classical calculations trace this phenomenon to transient decoupling of the molecule from its helium shell. Our results open novel opportunities for studying nonequilibrium solute-solvent dynamics and quantum thermalization.

DOI: 10.1103/PhysRevLett.118.203203

Usually, molecules dissolved in a liquid are not rotating freely due to the intermolecular forces exerted by the surrounding solvent. An important exception is molecules embedded in liquid helium nanodroplets where high-resolution infrared [1] and microwave [2] spectroscopies display discrete rotational structure. These observations along with theoretical modeling has established a picture that molecules inside helium nanodroplets can rotate without friction although followed by a local solvation shell of helium atoms. This shell increases the effective molecular moment of inertia compared to the gas-phase value [3,4].

These unique properties build the expectation that it should be possible to induce frictionless rotation of molecules inside helium droplets and follow it in real time. For isolated molecules versatile techniques based on moderately intense fs or ps laser pulses have been developed to control the rotational degrees of freedom [5–9]. In particular, such methods have been extensively used to confine molecular axes to laboratory-fixed axes—methods referred to as alignment and orientation [6]. Recently, the first time-resolved experiments of molecular rotation inside helium droplets revealed that moderately intense laser pulses can induce alignment of molecules [10,11]. The measurements showed, however, no sign of frictionless rotation. Notably, the transient alignment-recurrences (revivals) characteristic of freely rotating molecules in a gas phase were absent. These observations seemed at odds with the prevailing conception of rotational structure obtained through spectroscopy [3,4].

Here we experimentally demonstrate that a sufficiently weak fs pulse can initiate coherent rotation of iodine molecules together with their helium solvation shell–lasting long enough to form revivals. Our observations are rationalized by a quantum theory based on the angulon quasiparticle [12–18]. For strong alignment pulses the revivals disappear and, instead, strikingly fast rotational dynamics appears immediately after the pulse. Classical estimates indicate that, in this regime, helium atoms of the solvation shell detach from the molecule due to the centrifugal force generated by the rapid rotation. This can be seen as a sudden decoupling of the molecule from its solvent and for a short time the rotational motion resembles that of a free molecule.

In our experiment, 10-nm-diameter helium droplets—each doped with at most one iodine (I_2) molecule—are first irradiated by a 450 fs linearly polarized laser pulse at 800 nm. The purpose of this kick pulse is to induce alignment of the molecules, i.e., confine their I–I internuclear axis along the polarization direction [6]. Next, the molecules are Coulomb exploded by a delayed, intense probe pulse (40 fs, 3.7×10^{14} W/cm^2) which produces IHe$^+$ ion fragments with recoil directions given by the angular distribution of the molecular axes at the instant of the probe pulse. By detecting the emission directions of the IHe$^+$ ions with a 2D imaging detector at many different kick-probe delays, t, the time-dependent degree of alignment, $\langle\cos^2\theta_{2D}\rangle$, can be determined—$\theta_{2D}$ being the angle between the alignment pulse polarization and the projection of an IHe$^+$ ion velocity vector on the detector [19]. More details on the experimental setup are provided in the Supplemental Material [20], which includes Refs. [3,6,10,21,22].

Figure 1 shows $\langle\cos^2\theta_{2D}\rangle$ as a function of time for a series of different fluences of the kick pulse, F_{kick}. At low F_{kick} there is a distinct maximum in $\langle\cos^2\theta_{2D}\rangle$ shortly after the kick pulse [Figs. 1(a)–(d)]. The prompt peak grows in amplitude and appears earlier as F_{kick} is increased [Figs. 1(a2)–(d2)]. This behavior is the result of faster rotation and more efficient alignment induced by a stronger kick pulse and appears

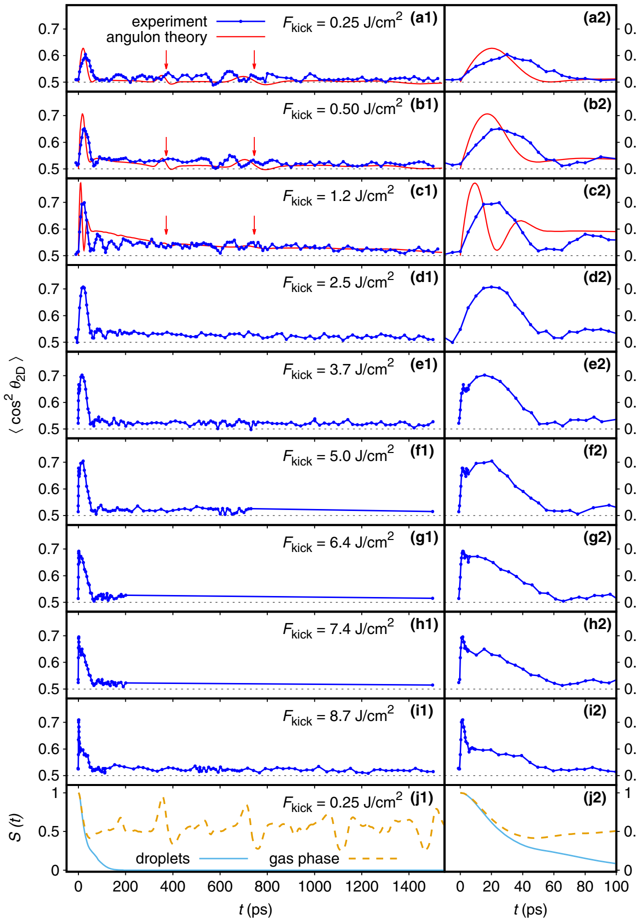

FIG. 1. The degree of alignment, $\langle \cos^2\theta_{2D}\rangle$, as a function of time at different fluences of the kick pulse (centered at $t = 0$); blue curves: experimental results; red curves: results from the angulon theory (revivals indicated by red arrows). In panel (f1) the time interval 750–1500 ps and in panels (g1) and (h1) the time interval 200–1500 ps are shown as straight lines because, for experimental reasons, $\langle \cos^2\theta_{2D}\rangle$ was not recorded in these regions. The right column of panels expands on the first 100 ps to highlight the structure that starts to appear at $F_{kick} = 3.7$ J/cm^2 immediately after the kick pulse and grows to a sharp peak with maximum at $t = 1.3$ ps for $F_{kick} = 8.7$ J/cm^2. Panels (j) show the survival probability of the initial state, as defined in the text.

similar to previous measurements on CH_3I molecules in helium droplets [10]. The current data exhibit, however, new, previously unobserved features. First, at $F_{kick} = 1.2$ J/cm^2 the prompt alignment peak is followed by pronounced yet decreasing oscillations out to ~200 ps. Second, for $F_{kick} = 0.25$, 0.50, and 1.2 J/cm^2 an oscillatory structure is observed in the interval 550–750 ps. The structure is very similar for the three fluences with local maxima and minima at essentially the same times. Third, on average the $\langle \cos^2\theta_{2D}\rangle$ curves are gradually decaying in the range ~100–1500 ps for $F_{kick} = 0.50$, 1.2, and 2.5 J/cm^2.

For $F_{kick} \geq 2.5$ J/cm^2 the structure in the 550–750 ps interval disappears. Also, the oscillations after the main peak are strongly reduced for $F_{kick} = 2.5$ J/cm^2 and essentially absent at larger fluences. Instead a substructure in the prompt alignment peak starts to appear at $F_{kick} = 3.7$ J/cm^2 [Fig. 1(e2)]. As the fluence is increased the substructure grows to a prominent sharp peak ending with a maximum already at $t \sim 1.3$ ps for $F_{kick} = 8.7$ J/cm^2 [Figs. 1(i) and 4].

We interpret the oscillations after the prompt peak and the 550–750 ps structure as manifestations of coherent rotation of the molecules and their local helium solvation shell—hereafter termed helium-dressed molecules. To substantiate this interpretation we first model helium-dressed molecules as classical rigid rotors driven by the polarizability interaction with the kick pulse. A helium-dressed molecule initially at an angle θ_0 to the kick pulse polarization [Fig. 2(a3)] gains an angular velocity, ω, of [23]:

$$\omega = \frac{1}{2}\frac{\Delta\alpha F_{kick}\sin(2\theta_0)}{I_{eff}\varepsilon_0 c}, \tag{1}$$

where $\Delta\alpha$ is the polarizability anisotropy of I_2 and I_{eff} is the effective moment of inertia of I_2 in the droplets. No experimental value exists for I_{eff} so we determined it by a path integral Monte Carlo calculation [24–27], which included all degrees of freedom, including molecule rotation, and the ^{4}He Bose symmetry (for details see the Supplemental Material [20], which includes Refs. [24,28–33]). This gave $I_{eff} = 1.7 \times I_0$ where I_0 is the moment of inertia of the bare I_2 molecule. The calculated helium density around the I_2 molecule is shown in Fig. 3. In our classical calculations a helium-dressed molecule is treated as an I_2 molecule rigidly

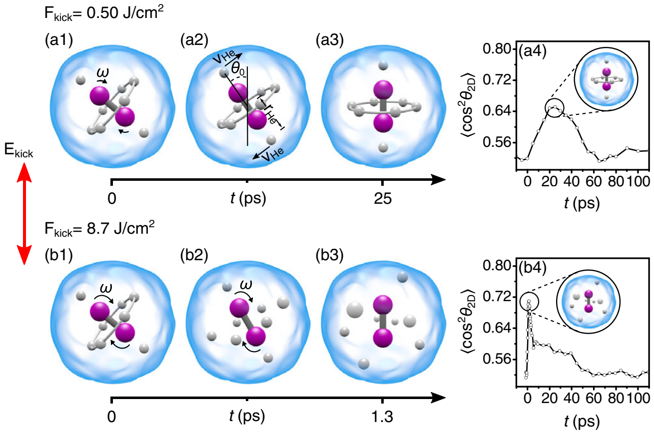

FIG. 2. Schematic illustration of laser-induced rotation of I_2 molecules inside helium droplets, based on the classical model described in the text, for a weak [(a1)–(a3)] and a strong [(b1)–(b3)] kick pulse. (a4) and (b4) relate the illustrations to the data recorded. (a2) illustrates parameters used in the classical model. θ_0: The angle between the molecular axis and the kick pulse polarization just prior to the laser-molecule interaction. r_{He}: Distance from the helium atom at the ends to the axis of rotation. v_{He}: The linear speed of the helium atoms at the ends of the molecule gained from the laser-molecule interaction.

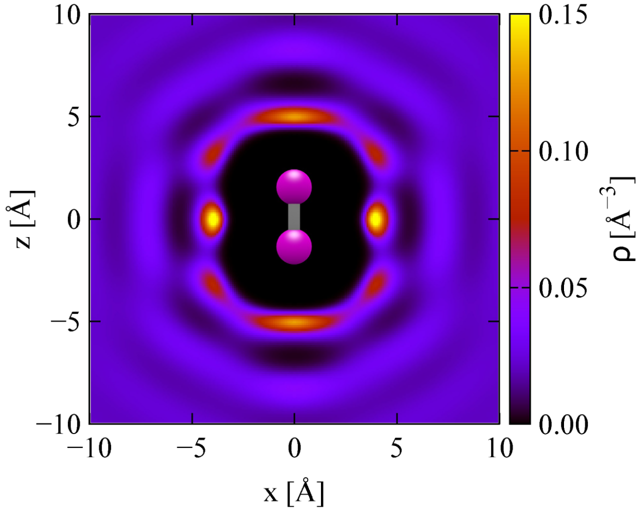

FIG. 3. Helium density, ρ, around I_2 in the molecular frame in equilibrium. It is obtained from a path integral Monte Carlo calculation [20] and corresponds to the situation prior to the kick pulse.

attached to eight helium atoms placed in the minima of the I_2–He potential [1,32] (six helium atoms in the central ring around the molecule and two at the ends); see Fig. 2. The value of I_{eff} determined from this structure (Fig. 2) is essentially equal to the Monte Carlo one.

Equation (1) predicts that the helium-dressed molecules are set into end-over-end rotation (Fig. 2) leading to a prompt alignment peak as observed experimentally. Continued rotation for extended times requires that superfluidity of the droplets is undistorted. A simple classical criterion for this is that the linear speed of the outer components of the helium-dressed molecules should not exceed the Landau velocity, $v_L = 56$ m/s [34]. The highest linear speed is calculated as $v_{\mathrm{He}} = \omega r_{\mathrm{He}}$, where r_{He} is the distance from a helium atom at the ends to the axis of rotation (see Fig. 2). Table I displays the values of ω and v_{He} for the nine different fluences used in the experiment. For $F_{\mathrm{kick}} = 0.25$ and $0.50\ \mathrm{J/cm^2}$ $v_{\mathrm{He}} < v_L$, whereas at $F_{\mathrm{kick}} = 1.2\ \mathrm{J/cm^2}$ v_{He} is just above v_L. At higher fluences, $v_{\mathrm{He}} \gg v_L$ for almost all of the helium-dressed molecules—independent of their initial orientation. These simple classical considerations indicate that long-time coherent rotational dynamics of the helium-dressed molecules is only possible for the three lowest fluences—in accordance with the observations—and illustrated by panels (a1)–(a3) of Fig. 2.

TABLE I. Classical calculation of the maximum angular velocity using Eq. (1) with $\theta_0 = 45°$ for the nine different fluences used in the experiment. From ω the linear speed, v_{He}, and the rotational energy, $E_{\mathrm{rot}}(\mathrm{He})$, of the helium atoms at the ends of the molecules are calculated; see text.

F_{kick}, $\mathrm{J/cm^2}$	ω, 10^{10} Hz	v_{He}, m/s	$E_{\mathrm{rot}}(\mathrm{He})$, $\mathrm{cm^{-1}}$
0.25	2.7	13	0.029
0.50	5.5	26	0.12
1.2	14	65	0.71
2.5	27	130	2.8
3.7	41	195	6.4
5.0	54	260	11
6.4	70	338	19
7.4	81	390	26
8.7	95	454	35

To elucidate the quantum dynamics of the system, we apply the recently developed angulon theory [13–18], which was shown to provide a reliable description for molecules in superfluid ^{4}He [12]. The details of the angulon theory are presented elsewhere [12–15]; here we outline the approximations involved in the treatment. The angulon theory describes the interaction of a rotating molecule with an infinite bath of bosonic degrees of freedom with a given dispersion relation [35]. The molecule-boson coupling is considered to be linear [13,14], with the coupling constants proportional to the anisotropy of the two-body potential energy surface [12,32]. We use the strong-coupling angulon theory [15], which applies when the following conditions take place. (i) $B_{\mathrm{eff}} \ll \sqrt{\alpha_1}$, where B_{eff} is the effective rotational constant in the presence of helium, and α_1 parametrizes the anisotropic molecule-helium interactions [20]. This was shown to be a fair approximation for I_2 molecules in helium droplets [12]. (ii) The molecule-laser interaction energy $\eta \lesssim \sqrt{\alpha_1}$. If this criterion is not satisfied, the molecule can detach from the surrounding helium atoms due to the laser pulse. To calculate the time evolution, we used the Suzuki-Trotter expansion [36] to order $\mathcal{O}(t^3(B_{\mathrm{eff}}\alpha_1 + B_{\mathrm{eff}}^2\sqrt{\alpha_1}))$.

The case of I_2 in helium belongs to the strong-coupling regime, where the molecular kinetic energy is small compared to the molecule-helium interactions [12]. In this regime, the angulon theory furnishes a closed-form expression for the alignment cosine:

$$
\begin{aligned}
&\langle\cos^2\hat{\theta}_{2\mathrm{D}}\rangle(t)\\
&\quad= \sum_{j,j',j_1,j_2,m} c^*_{j'} c_j e^{it(E_{j_2}+E_{j'}-E_{j_1}-E_j)/2}\langle j_2 m|\cos^2\hat{\theta}_{2D}|j_1 m\rangle\\
&\qquad\times\int d\Omega_1\int d\Omega_2 Y^*_{j'm_0}(\Omega_2)Y_{j_2 m}(\Omega_2)Y_{jm_0}(\Omega_1)Y^*_{j_1 m}(\Omega_1)\\
&\qquad\times e^{\alpha_1 t^2[(4\pi/5)\sum_\mu Y_{2,\mu}(\Omega_2)Y^*_{2,\mu}(\Omega_1)-1]} \qquad (2)
\end{aligned}
$$

(in units of $\hbar \equiv 1$), where $E_j = B_{\mathrm{eff}} j(j+1)$, and the coefficients, $c_j = \langle j, m_0|\exp(\eta\cos^2\hat{\theta})|j_0, m_0\rangle$, describe the rotational wave packet created from the initial molecular state $|j_0, m_0\rangle$ by a short laser pulse with a dimensionless intensity η. In order to compare the theory to experiment, the results of Eq. (2) were averaged over the thermal distribution of the initial states and the finite width of rotational lines due to dephasing was accounted for. More details on the theoretical approach are provided in the Supplemental Material [20], which includes Refs. [37–46].

The fluences shown in Figs. 1(a) and 1(b) correspond to $\eta/\sqrt{\alpha_1} \approx 1.4$ and 2.7, respectively, which justifies the strong-coupling angulon theory. Both calculated $\langle\cos^2\theta_{2D}\rangle$ curves (red) are dominated by a prominent peak at early times. For $F_{\rm kick} = 0.25$ and $0.50\ {\rm J/cm^2}$ the prompt alignment peak agrees with the experimental curves although the peak amplitude is somewhat higher for the calculated curves. We ascribe this to an underestimation of the measured degree of alignment due to nonaxial recoil effects in the Coulomb explosion process, caused by the helium environment [47]. The fluence of $F_{\rm kick} = 1.2\ {\rm J/cm^2}$ corresponds to $\eta/\sqrt{\alpha_1} \approx 7$ and therefore lies beyond the reach of the strong-coupling angulon theory which predicts a faster initial dynamics compared to the experiment. In particular, the theory predicts rapid oscillations of alignment at small times, similar to the gas phase (cf. Fig. 4), which is absent in the experiment. Nevertheless, the long-time decay of alignment observed experimentally is reproduced.

For $F_{\rm kick} = 0.25$ and $0.50\ {\rm J/cm^2}$ low-amplitude structures just before 400 and 800 ps are visible. The angulon model identifies these as the half and full revival of the helium-dressed molecule, marked by red arrows for the theoretical curves. The locations of the revival structures match $h/(4B_{\rm eff})$ and $h/(2B_{\rm eff})$, with $B_{\rm eff} = \hbar^2/(2I_{\rm eff})$, similar to the well-studied case of isolated molecules. The magnitude of the revivals decreases for larger fluences, and they are no longer visible for $F_{\rm kick} \geq 2.5\ {\rm J/cm^2}$.

Importantly, the angulon theory predicts that rotational revivals are possible for molecules strongly interacting with superfluid helium. Therefore, we interpret the observed oscillatory structure in the 550–750 ps interval as a full rotational revival of the helium-dressed molecule. We note that the position of the experimentally observed recurrence structure deviates from the positions of the calculated revivals. We attribute this discrepancy to the fact that in our model the rotational structure of a helium-dressed molecule is described by a single parameter $B_{\rm eff}$. To obtain a better agreement with the experiment including higher-order corrections to energy might be necessary [3]. Furthermore, we note that the model captures the overall decay of $\langle\cos^2\theta_{2D}\rangle$ observed most clearly for $F_{\rm kick} = 0.50$ and $1.2\ {\rm J/cm^2}$. We quantify this decay by the survival probability (closely related to the Loschmidt echo [48]), $S(t) = |\langle\psi(t)|\psi_0\rangle|^2 \equiv |\langle\psi_0|e^{iHt}|\psi_0\rangle|^2$, of the state $|\psi_0\rangle$ immediately after the kick pulse excitation during time evolution under the angulon Hamiltonian H [20]. The time dependence of the survival probability is shown in Fig. 1(j). While the gas-phase survival probability (dashed line) exhibits revivals similar to the gas-phase molecular alignment, for I_2 in helium we predict a Gaussian decay $S(t) \sim \exp(-\alpha_1 t^2)$ [20]. The latter comes from redistribution of the angular momentum between the molecule and the superfluid. Note that this decay occurs on a faster time scale compared to the exponential decay common for Markovian reservoirs [49].

In the high-fluence regime, $\eta/\sqrt{\alpha_1} \gg 1$, the strong-coupling angulon theory is not applicable. However, classically, a high-fluence pulse can induce such a fast rotation of the helium-dressed molecule that helium atoms detach due to the centrifugal force—a mechanism which, we believe, is responsible for the sharp structure appearing in the prompt alignment peak. A simple criterion for detaching one helium atom is $E_{\rm rot}({\rm He}) > E_{\rm binding}({\rm He})$, where $E_{\rm rot}({\rm He}) = \frac{1}{2}m_{\rm He}\, r_{\rm He}^2\omega^2$ is the rotational energy of a helium atom and $E_{\rm binding}({\rm He}) \approx 16\ {\rm cm^{-1}}$ is the ground-state binding energy of the HeI_2 complex [32,50]. Table I displays $E_{\rm rot}({\rm He})$ calculated for the different fluences. At $F_{\rm kick} \gtrsim 6\ {\rm J/cm^2}$ the criterion is met implying that one or indeed several helium atoms detach from the molecule (lower panels in Fig. 2) since the binding energies of the first few helium atoms are similar [51].

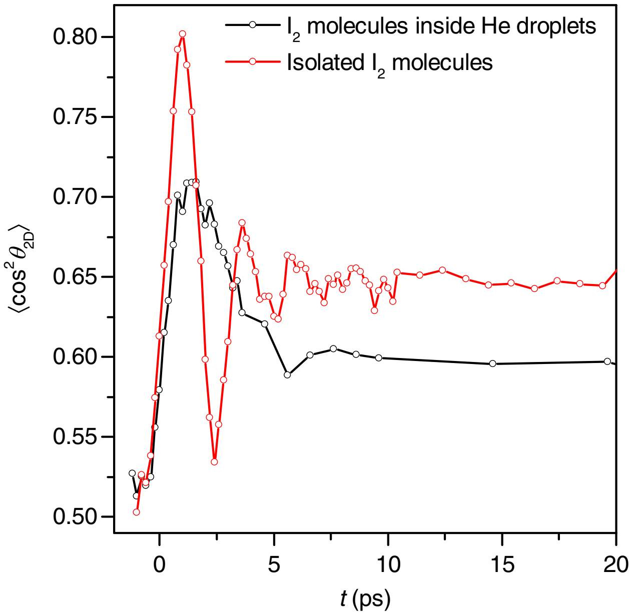

FIG. 4. The degree alignment, $\langle\cos^2\theta_{2D}\rangle$, at early times for isolated I_2 molecules and I_2 molecules in helium droplets recorded for $F_{\rm kick} = 8.7\ {\rm J/cm^2}$. The laser parameters of both the kick pulse and the probe pulse were identical for the measurements on the isolated molecules and on the molecules in helium droplets.

Figure 4 compares the short-time alignment dynamics of molecules in helium droplets to that of isolated molecules at $F_{\rm kick} = 8.7\ {\rm J/cm^2}$. In droplets, $\langle\cos^2\theta_{2D}\rangle$ evolves almost as fast as $\langle\cos^2\theta_{2D}\rangle$ of isolated molecules during the first ~2 ps. In classical terms, this indicates that I_2 rotates almost freely, detached from the helium atoms. We observed the same rapid short-time alignment dynamics for OCS and CS_2 molecules in helium droplets. At $t > 2$ ps the free rotation is quenched, which indicates a dynamical reformation of the helium-dressed molecule. It is important to note the absence of revivals for the results presented in Figs. 1(d)–(i), which indicates the loss of rotational coherence during the detachment-reattachment process.

Our results demonstrate that for molecules embedded in helium droplets a moderately intense laser pulse can induce coherent collective rotation of a molecule and its solvation shell for times long enough to form rotational revivals. These findings reconcile femtosecond laser-induced molecular alignment and high-resolution infrared and microwave spectroscopy. Our angulon quasiparticle theory rationalizes the observations for the low-fluence experimental results. Future generalization of the theory may lead to a quantitative agreement with experiments in a broad range of laser fluences and is expected to provide new insights into the superfluid behavior of helium droplets. Finally, the observed decoupling of the molecule from its helium-solvation shell at high fluences draws parallels to the nonlinear response in the solute-solvent interaction of rapidly rotating CN molecules dissolved in ethanol [52,53]. Our results open unique opportunities for real-time studies of nonequilibrium solute-solvent dynamics, for instance, by gradually modifying the solvation shell through insertion of other noble gas atoms or even water molecules [4]. Furthermore, experiments on molecules in small helium droplets might yield insight into quantum thermalization of finite many-particle systems [54,55].

We thank Richard Schmidt for insightful discussions. J. K. acknowledges support from People Programme (Marie Curie Actions) of the European Union's Seventh Framework Programme (FP7/2007–2013) under REA Grant Agreement No. [291734]. R. E. Z. acknowledges support from the Austrian Science Fund (FWF) under Grant No. P23535-N20. M. L. acknowledges support from the Austrian Science Foundation (FWF), under Grant No. P29902-N27. H. S. acknowledges support from the European Research Council-AdG (Project No. 320459, DropletControl) and the Villum Foundation.

---

[*] Robert.Zillich@jku.at
[†] mikhail.lemeshko@ist.ac.at
[‡] henriks@chem.au.dk

[1] S. Grebenev, M. Hartmann, M. Havenith, B. Sartakov, J. P. Toennies, and A. F. Vilesov, J. Chem. Phys. **112**, 4485 (2000).
[2] R. Lehnig, P. L. Raston, and W. Jäger, Faraday Discuss. **142**, 297 (2009).
[3] J. P. Toennies and A. F. Vilesov, Angew. Chem., Int. Ed. Engl. **43**, 2622 (2004).
[4] M. Y. Choi, G. E. Douberly, T. M. Falconer, W. K. Lewis, C. M. Lindsay, J. M. Merritt, P. L. Stiles, and R. E. Miller, Int. Rev. Phys. Chem. **25**, 15 (2006).
[5] L. Cai and B. Friedrich, Collect. Czech. Chem. Commun. **66**, 991 (2001).
[6] H. Stapelfeldt and T. Seideman, Rev. Mod. Phys. **75**, 543 (2003).
[7] Y. Ohshima and H. Hasegawa, Int. Rev. Phys. Chem. **29**, 619 (2010).
[8] M. Lemeshko, R. Krems, J. Doyle, and S. Kais, Mol. Phys. **111**, 1648 (2013).
[9] A. Korobenko, A. A. Milner, J. W. Hepburn, and V. Milner, Phys. Chem. Chem. Phys. **16**, 4071 (2014).
[10] D. Pentlehner, J. H. Nielsen, A. Slenczka, K. Mølmer, and H. Stapelfeldt, Phys. Rev. Lett. **110**, 093002 (2013).
[11] L. Christiansen, J. H. Nielsen, D. Pentlehner, J. G. Underwood, and H. Stapelfeldt, Phys. Rev. A **92**, 053415 (2015).
[12] M. Lemeshko, Phys. Rev. Lett. **118**, 095301 (2017).
[13] R. Schmidt and M. Lemeshko, Phys. Rev. Lett. **114**, 203001 (2015).
[14] M. Lemeshko and R. Schmidt, arXiv:1703.06753.
[15] R. Schmidt and M. Lemeshko, Phys. Rev. X **6**, 011012 (2016).
[16] E. Yakaboylu and M. Lemeshko, Phys. Rev. Lett. **118**, 085302 (2017).
[17] E. S. Redchenko and M. Lemeshko, ChemPhysChem **17**, 3649 (2016).
[18] X. Li, R. Seiringer, and M. Lemeshko, Phys. Rev. A **95**, 033608 (2017).
[19] A. A. Søndergaard, B. Shepperson, and H. Stapelfeldt, J. Chem. Phys. **147**, 013905 (2017).
[20] See Supplemental Material at http://link.aps.org/supplemental/10.1103/PhysRevLett.118.203203 for details.
[21] T. Seideman and E. Hamilton, Adv. At. Mol. Opt. Phys. **52**, 289 (2005).
[22] D. Pentlehner, J. H. Nielsen, L. Christiansen, A. Slenczka, and H. Stapelfeldt, Phys. Rev. A **87**, 063401 (2013).
[23] M. Leibscher, I. S. Averbukh, and H. Rabitz, Phys. Rev. A **69**, 013402 (2004).
[24] D. M. Ceperley, Rev. Mod. Phys. **67**, 279 (1995).
[25] Y. K. Kwon, D. M. Ceperley, and K. B. Whaley, J. Chem. Phys. **104**, 2341 (1996).
[26] N. Blinov, X. Song, and P.-N. Roy, J. Chem. Phys. **120**, 5916 (2004).
[27] R. E. Zillich, F. Paesani, Y. Kwon, and K. B. Whaley, J. Chem. Phys. **123**, 114301 (2005).
[28] R. P. Feynman and A. R. Hibbs, *Quantum Mechanics and Path Integrals*, International Series in Pure and Applied Physics (McGraw-Hill, New York, 1965).
[29] D. Chandler and P. G. Wolynes, J. Chem. Phys. **74**, 4078 (1981).
[30] M. Boninsegni, N. V. Prokofev, and B. V. Svistunov, Phys. Rev. E **74**, 036701 (2006).
[31] R. A. Aziz, F. R. W. McCourt, and C. C. K. Wong, Mol. Phys. **61**, 1487 (1987).
[32] L. García-Gutierrez, L. Delgado-Tellez, Á. Valdés, R. Prosmiti, P. Villarreal, and G. Delgado-Barrio, J. Phys. Chem. A **113**, 5754 (2009).
[33] N. Metropolis, A. W. Rosenbluth, M. N. Rosenbluth, A. H. Teller, and E. W. Teller, J. Chem. Phys. **21**, 1087 (1953).
[34] N. B. Brauer, S. Smolarek, E. Loginov, D. Mateo, A. Hernando, M. Pi, M. Barranco, W. J. Buma, and M. Drabbels, Phys. Rev. Lett. **111**, 153002 (2013).
[35] R. J. Donnelly and C. F. Barenghi, J. Phys. Chem. Ref. Data **27**, 1217 (1998).
[36] M. Suzuki, Commun. Math. Phys. **51**, 183 (1976).
[37] B. Midya, M. Tomza, R. Schmidt, and M. Lemeshko, Phys. Rev. A **94**, 041601(R) (2016).
[38] D. A. Varshalovich, A. Moskalev, and V. Khersonskii, *Quantum Theory of Angular Momentum* (World Scientific, Singapore, 1988).
[39] J. T. Devreese, arXiv:1012.4576.

[40] A. Leggett, S. Chakravarty, A. T. Dorsey, M. P. A. Fisher, A. Garg, and W. Zwerger, Rev. Mod. Phys. **59**, 1 (1987).
[41] R. Machleidt and D. Entem, Phys. Rep. **503**, 1 (2011).
[42] E. Fradkin, *Field Theories of Condensed Matter Physics*, 2nd ed. (Cambridge University Press, Cambridge, England, 2013).
[43] H. Lefebvre-Brion and R. W. Field, *The Spectra and Dynamics of Diatomic Molecules* (Elsevier, New York, 2004).
[44] L. C. Biedenharn and J. D. Louck, *Angular Momentum in Quantum Physics* (Addison-Wesley, Reading, MA, 1981).
[45] N. E. Henriksen, Chem. Phys. Lett. **312**, 196 (1999).
[46] R. E. Zillich, K. B. Whaley, and K. von Haeften, J. Chem. Phys. **128**, 094303 (2008).
[47] L. Christensen, L. Christiansen, B. Shepperson, and H. Stapelfeldt, Phys. Rev. A **94**, 023410 (2016).
[48] P. R. Zangara, A. D. Dente, P. R. Levstein, and H. M. Pastawski, Phys. Rev. A **86**, 012322 (2012).
[49] S. Ramakrishna and T. Seideman, Phys. Rev. Lett. **95**, 113001 (2005).
[50] S. E. Ray, A. B. McCoy, J. J. Glennon, J. P. Darr, E. J. Fesser, J. R. Lancaster, and R. A. Loomis, J. Chem. Phys. **125**, 164314 (2006).
[51] F. Paesani and K. B. Whaley, J. Chem. Phys. **121**, 4180 (2004).
[52] A. C. Moskun, A. E. Jailaubekov, S. E. Bradforth, G. Tao, and R. M. Stratt, Science **311**, 1907 (2006).
[53] G. Tao and R. M. Stratt, J. Chem. Phys. **125**, 114501 (2006).
[54] M. Rigol, V. Dunjko, and M. Olshanii, Nature (London) **452**, 854 (2008).
[55] A. Polkovnikov, K. Sengupta, A. Silva, and M. Vengalattore, Rev. Mod. Phys. **83**, 863 (2011).